

# Compact Superconducting Terahertz Source Operating in Liquid Nitrogen

L. Y. Hao,<sup>1</sup> M. Ji,<sup>1,2</sup> J. Yuan,<sup>2</sup> D. Y. An,<sup>1,2</sup> M. Y. Li,<sup>1,2</sup> X. J. Zhou,<sup>1,2</sup> Y. Huang,<sup>1,2</sup> H. C. Sun,<sup>1</sup> Q. Zhu,<sup>1</sup> F. Rudau,<sup>3</sup> R. Wieland,<sup>3</sup> N. Kinev,<sup>4</sup> J. Li,<sup>1,\*</sup> W. W. Xu,<sup>1,5</sup> B. B. Jin,<sup>1,5</sup> J. Chen,<sup>1,5</sup> T. Hatano,<sup>2</sup> V. P. Koshelets,<sup>4</sup> D. Koelle,<sup>3</sup> R. Kleiner,<sup>3,†</sup> H. B. Wang,<sup>1,2,5,‡</sup> and P. H. Wu<sup>1</sup>

<sup>1</sup>Research Institute of Superconductor Electronics, Nanjing University, Nanjing 210093, People's Republic of China

<sup>2</sup>National Institute for Materials Science, Tsukuba 3050047, Japan

<sup>3</sup>Physikalisches Institut and Center for Collective Quantum Phenomena in LISA<sup>+</sup>, Universität Tübingen, D-72076 Tübingen, Germany

<sup>4</sup>Kotel'nikov Institute of Radio Engineering and Electronics, 125009 Moscow, Russia

<sup>5</sup>Cooperative Innovation Centre of Terahertz Science, Chengdu 610054, People's Republic of China  
(Received 3 November 2014; revised manuscript received 24 December 2014; published 19 February 2015)

We report on a liquid-nitrogen-cooled compact source for continuous terahertz (THz) emission. The emitter is a  $\text{Bi}_2\text{Sr}_2\text{CaCu}_2\text{O}_{8+\delta}$  intrinsic Josephson-junction stack embedded between two gold layers and sandwiched between two MgO substrates. The radiation is emitted to free space through a hollow metallic tube acting as a waveguide. The maximum emission power is  $1.17 \mu\text{W}$ . The tunable emission frequency bandwidth is up to 100 GHz with a maximum emission power at 0.311 THz. Since the operation voltage is about 1 V and the current is less than 30 mA, we are able to drive this terahertz source at 77 K with only one commercial 1.5-V battery, just like a torch. This convenient and economical setup may find applications in fields like tracer-gas detection or nondestructive evaluation.

DOI: 10.1103/PhysRevApplied.3.024006

## I. INTRODUCTION

Terahertz (THz) radiation covers the region from 0.3 THz (submillimeter) to 3 THz (far infrared) and is attracting increasing attention due to the variety of potential applications, including information and communication technology, biology and medical sciences, nondestructive evaluation, astronomical observation, and security [1–3]. The critical technical requirements are to develop powerful terahertz sources with certain features for different applications. One of the tasks is to develop compact and economical terahertz sources operated in a continuous-wave (cw) mode. Terahertz radiation for frequencies above 2 THz can be well generated using quantum cascade lasers. For frequencies below 1 THz, stacks of intrinsic Josephson junctions (IJJs) [4] in the high-transition-temperature ( $T_c$ ) superconductor  $\text{Bi}_2\text{Sr}_2\text{CaCu}_2\text{O}_{8+\delta}$  (BSCCO) have been shown to emit continuous and coherent radiation [5], with the possibility to tune the emitted frequency  $f_e$  by an applied dc voltage  $V$ , following the relation  $f_e = V/N\Phi_0$ . Here,  $\Phi_0$  is the flux quantum, with  $\Phi_0^{-1} \approx 483.6 \text{ GHz/mV}$ .  $N$  is the number of IJJs in the stack, and  $V/N$  is the voltage per junction. In Ref. [5], stacks of about  $1 \mu\text{m}$  in thickness (corresponding to 666 IJJs), a length  $L_s$  of about  $300 \mu\text{m}$ , and a width  $W$  of some  $10 \mu\text{m}$  have been realized as mesa structures on top of BSCCO single crystals contacted by

Au layers. These mesas emitted radiation at frequencies between 0.5 and 0.8 THz, with an integrated output power on the order of  $1 \mu\text{W}$ . The operation temperature was up to 50 K.

Terahertz radiation emitted from such IJJ stacks has become a hot topic in recent years [6–45]. The possibility to perform terahertz imaging has been demonstrated [22,40,41]. IJJ stacks containing typically 500–2000 junctions have been realized as mesa structures but also as bare IJJ stacks contacted by Au layers [gold-BSCCO-gold (GBG) structures] [28,30,36,38,43] and as all-superconducting Z-shaped structures [27]. Emission frequencies are in the range of 0.4–1 THz. For the best stacks—particularly, the GBG structures—emission powers in the range of tens of microwatts have been achieved [30,33,36], and arrays of stacks showed emission with a power up to 0.61 mW [33]. Both above-mentioned terahertz sources require cooling by liquid helium or by using cooling systems such as a Gifford-McMahon cryocooler or a Stirling cryocooler. In view of the applications, these cryogenic systems are inconvenient because of large equipment volume, electromagnetic noise, and mechanical vibrations [46,47].

Quite recently, attempts were reported to enhance the emission frequency to 1.05 THz and the tunable frequency range to more than 0.71 THz [43,45]. Particularly, in Ref. [43], the terahertz emission was observed at temperatures above 78 K, which allows the investigation and application of terahertz technology using liquid-nitrogen cooling.

\*junli@nju.edu.cn

†kleiner@uni-tuebingen.de

‡hbwang1000@gmail.com

In the present work, we report on a portable and tunable terahertz source operated in liquid nitrogen, which can provide cw terahertz emission. The GBG structure sandwiched between two MgO substrates is utilized as the terahertz emitter. The terahertz emission can be transmitted to free space through a metal tube acting as a waveguide. For a proof of principle, we also operate our source like a torch, with only one commercial 1.5-V battery.

## II. EXPERIMENTAL SETUP

The fabrication of the sandwiched GBG structure shown in Fig. 1(b) is described in Ref. [43]. The  $230 \times 50 \mu\text{m}^2$  BSCCO IJJ stack is  $1.5 \mu\text{m}$  thick and consists of approximately 1000 junctions. The single crystals used are optimally doped with  $T_c \sim 88 \text{ K}$ , which is the key factor for operating the device at liquid-nitrogen temperatures. In this GBG structure, the top gold layer can reflect the radiation of the IJJ stack to the MgO-1 substrate and then to a sapphire lens, enhancing the detectable emission power. We put another MgO substrate (MgO-2) on the top of the

GBG structure to form a sandwich structure, using polyimide (polyimide-1) as glue and a thermal anchor. At a given bias current  $I$  and a given bath temperature  $T$ , the total voltage  $V$  across the stack as well as the terahertz emission frequencies are significantly increased compared to the GBG structure mounted to a single substrate [43].

A photograph of the terahertz source is shown in the inset of Fig. 1(a). It consists of a copper container for holding the BSCCO emitter and a stainless-steel tube acting as a waveguide. Some pieces of black polyethylene films are employed on the outport of the waveguide to filter out some of the infrared background. An inside view of the copper container is presented in Fig. 1(a). The BSCCO emitter is fixed on a hemispherical sapphire lens with a 6 mm diameter. The terahertz waves are focused by the lens and then transmitted outward through the inner polished tube being a hollow circular waveguide with length of 180 mm and inner radius  $r = 1.75 \text{ mm}$ . We also place an  $R_{\text{heat}} = 1 \text{ k}\Omega$  heating resistor (heater) next to the lens to adjust the ambient temperature and, consequently, to expand the tunable frequency bandwidth.

## III. RESULTS AND DISCUSSION

For a hollow metallic circular waveguide, the cutoff frequencies  $f_c$  of transverse magnetic (TM) and transverse electric (TE) waves are, respectively,

$$(f_c)_{np}^{\text{TM}} = \frac{cx_{np}}{2\pi r}, \quad (1)$$

$$(f_c)_{np}^{\text{TE}} = \frac{cx'_{np}}{2\pi r}, \quad (2)$$

where  $x_{np}$  and  $x'_{np}$  represent the  $p$ th roots of the  $n$ th-order Bessel functions and its derivatives, respectively;  $c$  is the speed of light. Then,  $f_c$  of the main mode  $\text{TE}_{11}$  is 50 GHz and, thus, far below the operating frequency. Therefore, for the tunable frequency range from 0.266 to 0.364 THz, there are multiple transmission modes, among which the one having the highest cutoff frequency is  $\text{TE}_{24}$  with  $f_c = 0.359 \text{ THz}$ . The hollow circular waveguide transmits waves by bouncing them with the inner metallic surface; however, more reflections induce larger insertion losses [48,49]. By polishing the inner surface, the losses are reduced. Via simulation, the insertion loss  $L_I$  of the waveguide is estimated as about 10 dB according to the relation  $L_I = -20\log_{10}|S_{12}|(\text{dB})$ , where  $S_{12}$  is the transmission coefficient of the scattering matrix.

The power and the frequency (wavelength) of the terahertz emission are measured with a homemade Michelson interferometer armed with a Si bolometer. The power measurement is calibrated by a blackbody radiation source. The ratio between the power and the bolometer readout is  $2.1 \times 10^{-3} \text{ W/V}$ . For the fast Fourier transform, the frequency resolution of the Michelson

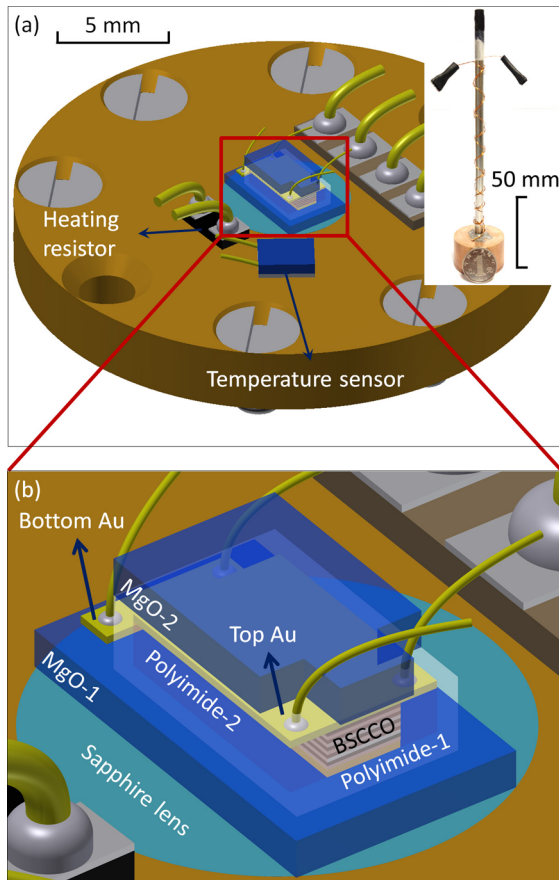


FIG. 1. Structure of the terahertz source. The inset in (a) is a photograph of the probe consisting of a stainless-steel tube acting as a waveguide and a hollow copper container hosting the emitter. The inner top part of the container is sketched upside down in (a). A close-up of the sandwiched GBG structure is shown in (b).

interferometer is given by  $\Delta f = c/(2d_{\max}) \cos(\theta)$ , where  $d_{\max}$  is the maximum differential displacement of the lamellar mirrors and  $\theta$  the angle of incidence [50]. In our setup,  $d_{\max} = 20$  mm and  $\theta \sim 0^\circ$ ; therefore,  $\Delta f$  can be estimated as 7.5 GHz. When the interferometer is inserted, the detected power is a factor of 4.3 lower than for direct bolometric detection.

Figure 2(a) shows a series of current-voltage characteristics (IVCs) for different temperatures ranging from the liquid-nitrogen boiling temperature (77 K) to the  $T_c$  (88 K) of the BSCCO emitter. The temperature of the emitter is varied using the heating resistor mounted on the copper container. The contact resistance  $R_{\text{cont}}$  from 2.1 to 4.6  $\Omega$  is subtracted from the IVC for each temperature. As shown in Fig. 2(a) by the horizontal dashed arrows, at 77 K all junctions have switched from the zero-voltage states to the resistive states when the bias current  $I > 20$  mA. By further increasing  $I$  to 24 mA and then sweeping it down, the IVC is continuous until some of the IJJs in the stack retrap to their zero-voltage states at the retrapping current  $I_r$  (11 mA at 77 K). The highest voltage across the mesa is

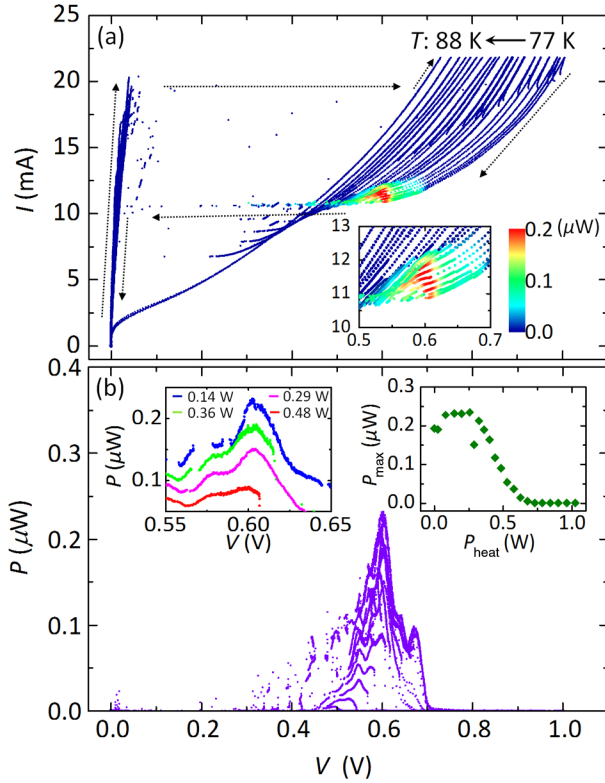


FIG. 2. IVCs and emission power (with interferometer inserted) obtained from the terahertz source for different temperatures  $T$ . The color contours represent different terahertz emission powers. (a) A series of IVCs. Dashed arrows denote the current sweep direction. The inset is a close-up of the emission region. (b) Emission power  $P$  as a function of the voltage  $V$  across the mesa. The right inset shows the maximum emission power  $P_{\max}$  vs the heater power  $P_{\text{heat}}$ . The left inset shows  $P$  vs  $V$  on a magnified voltage scale for four different values of  $P_{\text{heat}}$ .

observed as 1 V at 77 K. Different from the typical heat-induced S-shaped curves at relatively low temperatures, the IVCs are always monotonic above the liquid-nitrogen temperature. With increasing temperature (heater power  $P_{\text{heat}}$ ), the retrapping voltage is gradually decreasing, and the entire emission regime shifts to lower voltages, i.e., lower emission frequencies. When  $P_{\text{heat}}$  reaches 0.73 W, no emission can be detected anymore. When  $P_{\text{heat}}$  is increased to 1.0 W, the BSCCO stack goes normal; i.e., it reaches  $T_c = 88$  K.

The emission region covers a current range from about 11 to 12.5 mA and, correspondingly, a voltage range from 0.5 to 0.7 V, as shown in the inset of Fig. 2(a). The maximum emission power is observed around 0.6 V, corresponding to 0.311 THz at most temperatures; cf. Fig. 2(b). As shown in more detail in the right inset of this graph, the power peak is about  $0.23 \mu\text{W}$  at  $P_{\text{heat}} = 0.26$  W and  $0.19 \mu\text{W}$  at  $P_{\text{heat}} = 0$ . The highest value is  $0.27 \mu\text{W}$  at  $P_{\text{heat}} = 0.20$  W. These numbers are recorded via the Michelson interferometer and for  $P_{\text{heat}} = 0.20$  W ( $P_{\text{heat}} = 0$ ) correspond to  $1.17 \mu\text{W}$  ( $1.08 \mu\text{W}$ ) with direct bolometric detection.

In addition to the output power, the linewidth and the frequency tunability are important parameters for terahertz sources. Figure 3 shows at  $P_{\text{heat}} = 0.20$  W emission spectra taken at the four bias points marked on the IVC in the inset. The full width at half maximum of the emission peak at 0.311 THz is 7.5 GHz, which is the resolution limit of the interferometer. We do not perform high-resolution measurements of the emission peak using a superconducting receiver [24], but note that, at least for the IJJ emitters investigated previously, the linewidth of radiation can be as narrow as 23 MHz [24,35].

Figure 4(a) shows the tunability of the emission frequency with the bias current indicated by vertical error bars at a given bath temperature. For instance, at  $P_{\text{heat}} = 0.20$  W, it

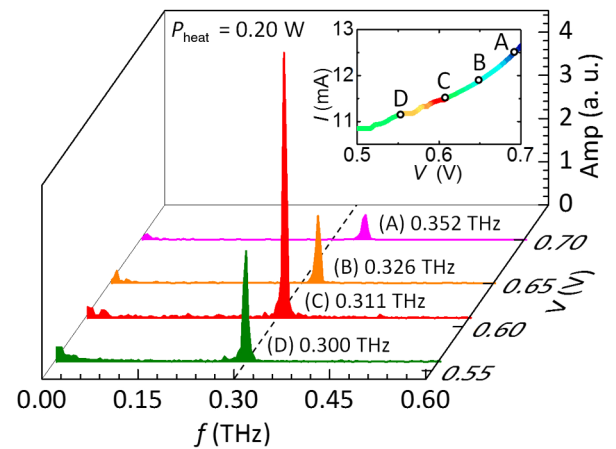


FIG. 3. Emission spectra at  $P_{\text{heat}} = 0.20$  W of the four bias points marked on the IVC shown in the inset. The colors in the main panel are used to distinguish different spectra, whereas the color mapping in the inset corresponds to that in Fig. 2(a).

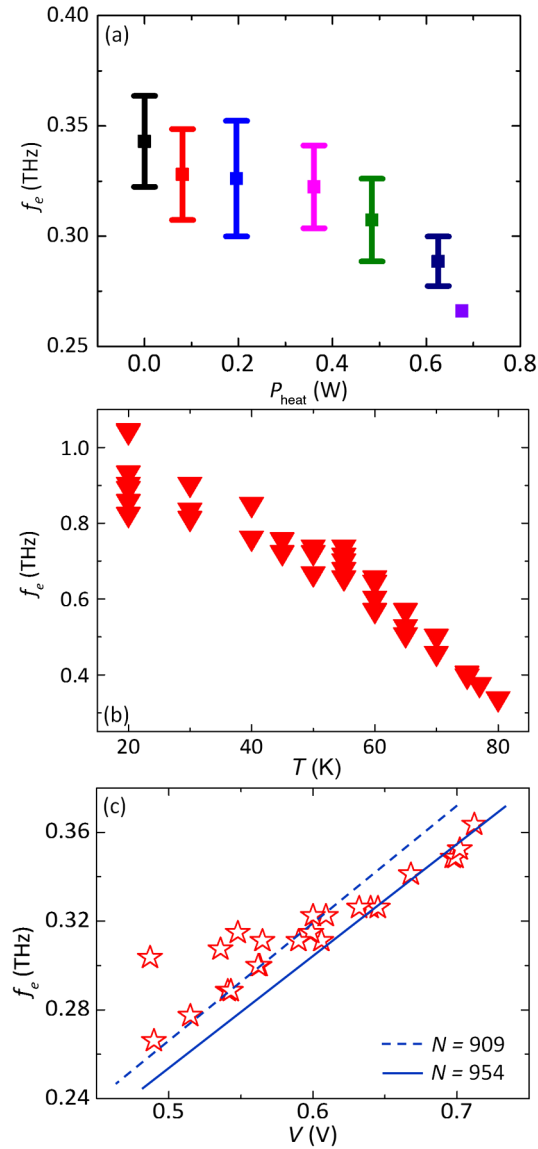


FIG. 4. (a) Frequency intervals of detectable emission vs the heater power  $P_{\text{heat}}$ . (b) Emission frequency  $f_e$  vs temperature  $T$  over a large temperature range up to 80 K, as measured with another setup [43]. (c) Emission frequency  $f_e$  vs voltage  $V$  across the mesa. The dashed and solid lines correspond to  $V = Nf_e\Phi_0$  with  $N = 909$  and  $954$ , respectively.

amounts to 52.5 GHz with the maximum emission power at 0.311 THz. The emission frequency can also be tuned with the temperature, which in our setup, we vary using a resistor placed next to the sample. Figure 4(a) shows the resulting temperature and frequency changes for seven values of the heater power  $P_{\text{heat}}$ . The total tunable frequency range is as broad as 100 GHz, which makes it possible to have certain applications like spectrum analysis of materials.

Note that the fact that  $f_e$  decreases strongly with the temperature is consistent with the assumption that in-plane supercurrents via cavity resonances are important for synchronization [3]. These currents lead to a large kinetic

inductance which diverges at  $T_c$ , and, consequently, the (in-phase) cavity mode velocity becomes small [9]. By contrast, a temperature independence of  $f_e$  would have suggested that in-plane currents dominantly flow in the gold layers, which does not seem to be the case at least for the GBG structure we use here.

In Fig. 4(c), for the measurements performed in liquid nitrogen, we plot  $f_e$  vs the voltage across the stack  $V$ . From the trend of the linear voltage dependence, we plot two fit lines,  $N = 909$  and  $954$ , which determine a range for the number of the active junctions that have contributed to the emission. There are some deviating data points. The reason is that some of the junctions in the stack have already switched back to the superconducting state. Thus, the voltage state turns to the inner branches of the IVC. The change in the number  $N$  of radiating junctions leads to a change in slope of the  $f_e$  vs  $V$  relation. For a given voltage, one observes a higher value of  $f_e$ , as described by Tsujimoto *et al.* [29].

To obtain a more portable and economical system, for a proof of principle, we also operate our terahertz source like a terahertz torch driven by a commercial battery. This operation is possible, since the maximum voltage is about 1 V and the current less than 30 mA. A 1.5-V battery is used as a voltage source, and two potentiometers with different resistors are utilized to adjust the output bias voltage. One of the potentiometers is 10 k $\Omega$  for coarse adjustment and the other is 100  $\Omega$  for fine adjustment. The current is obtained via a 10- $\Omega$  sampling resistor. Figure 5 shows an IVC and the emitted power for this operation mode.

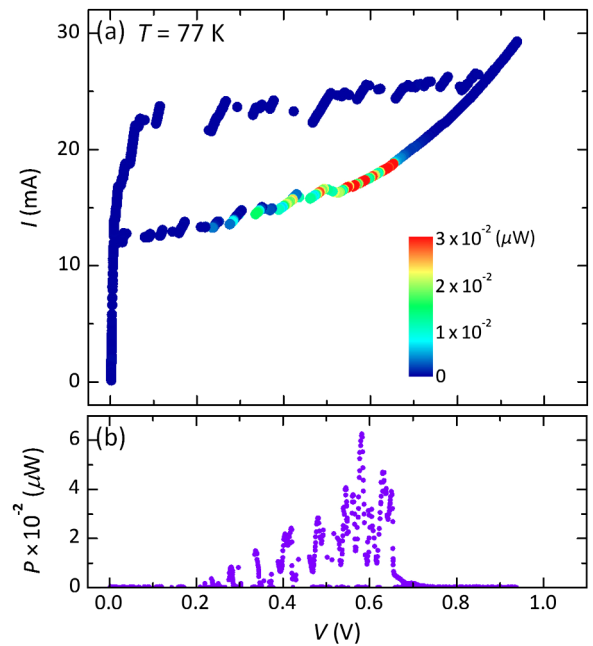


FIG. 5. Characteristics of the terahertz emitter ( $T = 77$  K) when operated with a 1.5-V battery. (a) IVC and (b) emitted power  $P$  vs voltage  $V$ .

The maximum emission power measured with the interferometer is only about  $0.063 \mu\text{W}$ , yielding  $0.27 \mu\text{W}$  for direct detection. However, we note that the device is not optimized for this kind of operation; thus, an increase of the emitted power  $P$  will certainly be feasible.

Finally, let us say a few words why our terahertz source can work at such a high temperature. At least two important factors may contribute to the high-temperature operation. One is to diffuse the Joule heating efficiently. In conventional mesa structures, an IJJ stack is located on a thick BSCCO base crystal, through which the heat diffuses from the mesa to the substrate. In a GBG structure, the thick BSCCO base crystal is replaced by a gold layer glued on a substrate by polyimide inducing a better heating transfer. The sandwich structure further improves the cooling because the IJJ stack is wrapped with polyimide (having a reasonably high thermal conductivity) on the periphery resulting in more contact areas with the copper holder [36,43]. The other important factor to achieve maximum operation temperature is that the crystal is close to optimal doping. Note that, in general, the precise temperature dependence of the  $c$ -axis resistivity, which, in turn, depends strongly on doping [51], strongly affects the thermal and electrodynamic properties of an IJJ stack [19,26,35]. Most previous results on terahertz generation by intrinsic junctions have been obtained with slightly underdoped crystals. The results presented in our paper show that terahertz generation is also feasible using optimally doped stacks, allowing us to operate IJJ stacks as terahertz sources in liquid nitrogen.

#### IV. CONCLUSION

In summary, we design and investigate a portable and tunable terahertz radiation system for continuous-wave terahertz emission. The coolant is liquid nitrogen. The terahertz waves are transmitted to free space through a metal tube acting as a waveguide. We demonstrate that the power source can be a commercial 1.5-V battery, allowing the operation as a “terahertz torch.” Along with satisfactory spectrum characteristics, the emission frequency is detected in the range of 0.266 to 0.364 THz. In virtue of its portability and frequency tunability, the system can be employed in practical applications. For example, for spectroscopy purposes, one can connect another tube containing some gas to the end of the waveguide. A terahertz detector can be attached easily to the end of this setup.

#### ACKNOWLEDGMENTS

This research is partly supported by the National Basic Research Program of China (973 Program) (Grants No. 2014CB339800 and No. 2011CBA00100), the National Natural Science Foundation of China (Grants No. 11234006, No. 51102188, No. 6127008, No. 2011CBA00107, and No. 11227904), the Fundamental Research Funds

for the Central Universities and Jiangsu Key Laboratory of Advanced Techniques for Manipulating Electromagnetic Waves, the China Academy of Engineering Physics (CAEP) THz Science and Technology Foundation (Grant No. CAEP THZ201202), the Russian Foundation for Basic Research (RFBR) (Grants No. 13-02-00493-a and 14-02-91335) and the Ministry of Education and Science of the Russian Federation (Grant No. 14.607.21.0100), the Japan Science and Technology/Deutsche Forschungsgemeinschaft (JST/DFG) strategic Japanese-German International Cooperative Program, Project No. KL930/12-1 of the Deutsche Forschungsgemeinschaft, the Grants-in-Aid for scientific research from Japan Society for the Promotion of Science (JSPS) (Grant No. 25289108), and the Priority Academic Program Development of Jiangsu Higher Education Institutions (PAPD).

- 
- [1] M. Tonouchi, Cutting-edge terahertz technology, *Nat. Photonics* **1**, 97 (2007).
  - [2] B. Ferguson and X. C. Zhang, Materials for terahertz science and technology, *Nat. Mater.* **1**, 26 (2002).
  - [3] U. Welp, K. Kadowaki, and R. Kleiner, Superconducting emitters of THz radiation, *Nat. Photonics* **7**, 702 (2013).
  - [4] R. Kleiner, F. Steinmeyer, G. Kunkel, and P. Müller, Intrinsic Josephson Effects in  $\text{Bi}_2\text{Sr}_2\text{CaCu}_2\text{O}_8$  Single Crystals, *Phys. Rev. Lett.* **68**, 2394 (1992).
  - [5] L. Ozyuzer, A. E. Koshelev, C. Kurter, N. Gopalsami, Q. Li, M. Tachiki, K. Kadowaki, T. Yamamoto, H. Minami, H. Yamaguchi, T. Tachiki, K. E. Gray, W.-K. Kwok, and U. Welp, Emission of coherent THz radiation from superconductors, *Science* **318**, 1291 (2007).
  - [6] S. Z. Lin and X. Hu, Possible Dynamic States in Inductively Coupled Intrinsic Josephson Junctions of Layered High- $T_c$  Superconductors, *Phys. Rev. Lett.* **100**, 247006 (2008).
  - [7] A. E. Koshelev, Alternating dynamic state self-generated by internal resonance in stacks of intrinsic Josephson junctions, *Phys. Rev. B* **78**, 174509 (2008).
  - [8] C. Kurter, K. E. Gray, J. F. Zasadzinski, L. Ozyuzer, A. E. Koshelev, Q. Li, T. Yamamoto, K. Kadowaki, W.-K. Kwok, M. Tachiki, and U. Welp, Thermal management in large  $\text{Bi}2212$  mesas used for terahertz sources, *IEEE Trans. Appl. Supercond.* **19**, 428 (2009).
  - [9] H. B. Wang, S. Guénon, J. Yuan, A. Iishi, S. Arisawa, T. Hatano, T. Yamashita, D. Koelle, and R. Kleiner, Hot Spots and Waves in  $\text{Bi}_2\text{Sr}_2\text{CaCu}_2\text{O}_8$  Intrinsic Josephson Junction Stacks: A Study by Low Temperature Scanning Laser Microscopy, *Phys. Rev. Lett.* **102**, 017006 (2009).
  - [10] M. Tachiki, S. Fukuya, and T. Koyama, Mechanism of Terahertz Electromagnetic Wave Emission from Intrinsic Josephson Junctions, *Phys. Rev. Lett.* **102**, 127002 (2009).
  - [11] N. F. Pedersen and S. Madsen, THz generation using fluxon dynamics in high temperature superconductors, *IEEE Trans. Appl. Supercond.* **19**, 726 (2009).
  - [12] A. E. Koshelev, Stability of dynamic coherent states in intrinsic Josephson-junction stacks near internal cavity resonance, *Phys. Rev. B* **82**, 174512 (2010).

- [13] S. Z. Lin and X. Hu, Response and amplification of terahertz electromagnetic waves in intrinsic Josephson junctions of layered high- $T_c$  superconductor, *Phys. Rev. B* **82**, 020504 (2010).
- [14] M. Tsujimoto, K. Yamaki, K. Deguchi, T. Yamamoto, T. Kashiwagi, H. Minami, M. Tachiki, K. Kadowaki, and R. A. Klemm, Geometrical Resonance Conditions for THz Radiation from the Intrinsic Josephson Junctions in  $\text{Bi}_2\text{Sr}_2\text{CaCu}_2\text{O}_{8+\delta}$ , *Phys. Rev. Lett.* **105**, 037005 (2010).
- [15] H. B. Wang, S. Guénon, B. Gross, J. Yuan, Z. G. Jiang, Y. Y. Zhong, M. Grünzweig, A. Iishi, P. H. Wu, T. Hatano, D. Koelle, and R. Kleiner, Coherent Terahertz Emission of Intrinsic Josephson Junction Stacks in the Hot Spot Regime, *Phys. Rev. Lett.* **105**, 057002 (2010).
- [16] S. Guénon, M. Grünzweig, B. Gross, J. Yuan, Z. G. Jiang, Y. Y. Zhong, M. Y. Li, A. Iishi, P. H. Wu, T. Hatano, R. G. Mints, E. Goldobin, D. Koelle, H. B. Wang, and R. Kleiner, Interaction of hot spots and terahertz waves in  $\text{Bi}_2\text{Sr}_2\text{CaCu}_2\text{O}_8$  intrinsic Josephson junction stacks of various geometry, *Phys. Rev. B* **82**, 214506 (2010).
- [17] V. M. Krasnov, Coherent flux-flow emission from stacked Josephson junctions: Nonlocal radiative boundary conditions and the role of geometrical resonances, *Phys. Rev. B* **82**, 134524 (2010).
- [18] V. M. Krasnov, Terahertz electromagnetic radiation from intrinsic Josephson junctions at zero magnetic field via breather-type self-oscillations, *Phys. Rev. B* **83**, 174517 (2011).
- [19] A. Yurgens, Temperature distribution in a large  $\text{Bi}_2\text{Sr}_2\text{CaCu}_2\text{O}_{8+\delta}$  mesa, *Phys. Rev. B* **83**, 184501 (2011).
- [20] T. M. Benseman, A. E. Koshelev, K. E. Gray, W.-K. Kwok, U. Welp, K. Kadowaki, M. Tachiki, and T. Yamamoto, Tunable terahertz emission from  $\text{Bi}_2\text{Sr}_2\text{CaCu}_2\text{O}_{8+\delta}$  mesa devices, *Phys. Rev. B* **84**, 064523 (2011).
- [21] T. Koyama, H. Matsumoto, M. Machida, and Y. Ota, Multi-scale simulation for terahertz wave emission from the intrinsic Josephson junctions, *Supercond. Sci. Technol.* **24**, 085007 (2011).
- [22] M. Tsujimoto, H. Minami, K. Delfanzari, M. Sawamura, R. Nakayama, T. Kitamura, T. Yamamoto, T. Kashiwagi, T. Hattori, and K. Kadowaki, Terahertz imaging system using high- $T_c$  superconducting oscillation devices, *J. Appl. Phys.* **111**, 123111 (2012).
- [23] S. Z. Lin and X. Hu, In-plane dissipation as a possible synchronization mechanism for terahertz radiation from intrinsic Josephson junctions of layered superconductors, *Phys. Rev. B* **86**, 054506 (2012).
- [24] M. Y. Li, J. Yuan, N. V. Kinev, J. Li, B. Gross, S. Guénon, A. Ishii, K. Hirata, T. Hatano, D. Koelle, R. Kleiner, V. P. Koshelets, H. B. Wang, and P. H. Wu, Linewidth dependence of coherent terahertz emission from  $\text{Bi}_2\text{Sr}_2\text{CaCu}_2\text{O}_8$  intrinsic Josephson junction stacks in the hot-spot regime, *Phys. Rev. B* **86**, 060505(R) (2012).
- [25] I. Takeya, Y. Omukai, T. Yamamoto, K. Kadowaki, and M. Suzuki, Effect of thermal inhomogeneity for terahertz radiation from intrinsic Josephson junction stacks of  $\text{Bi}_2\text{Sr}_2\text{CaCu}_2\text{O}_{8+\delta}$ , *Appl. Phys. Lett.* **100**, 242603 (2012).
- [26] B. Gross, S. Guénon, J. Yuan, M. Y. Li, J. Li, A. Ishii, R. G. Mints, T. Hatano, P. H. Wu, D. Koelle, H. B. Wang, and R. Kleiner, Hot-spot formation in stacks of intrinsic Josephson junctions in  $\text{Bi}_2\text{Sr}_2\text{CaCu}_2\text{O}_8$ , *Phys. Rev. B* **86**, 094524 (2012).
- [27] J. Yuan, M. Y. Li, J. Li, B. Gross, A. Ishii, K. Yamaura, T. Hatano, K. Hirata, E. Takayama-Muromachi, P. H. Wu, D. Koelle, R. Kleiner, and H. B. Wang, Terahertz emission from  $\text{Bi}_2\text{Sr}_2\text{CaCu}_2\text{O}_{8+\delta}$  intrinsic Josephson junction stacks with all-superconducting electrodes, *Supercond. Sci. Technol.* **25**, 075015 (2012).
- [28] T. Kashiwagi, M. Tsujimoto, T. Yamamoto, H. Minami, K. Yamaki, K. Delfanzari, K. Deguchi, N. Orita, T. Koike, R. Nakayama, T. Kitamura, M. Sawamura, S. Hagino, K. Ishida, K. Ivancovic, H. Asai, M. Tachiki, R. A. Klemm, and K. Kadowaki, High temperature superconductor terahertz emitters: Fundamental physics and its applications, *Jpn. J. Appl. Phys.* **51**, 010113 (2012).
- [29] M. Tsujimoto, T. Yamamoto, K. Delfanzari, R. Nakayama, T. Kitamura, M. Sawamura, T. Kashiwagi, H. Minami, M. Tachiki, K. Kadowaki, and R. A. Klemm, Broadly Tunable Subterahertz Emission from Internal Branches of the Current-Voltage Characteristics of Superconducting  $\text{Bi}_2\text{Sr}_2\text{CaCu}_2\text{O}_{8+\delta}$  Single Crystals, *Phys. Rev. Lett.* **108**, 107006 (2012).
- [30] S. Sekimoto, C. Watanabe, H. Minami, T. Yamamoto, T. Kashiwagi, R. A. Klemm, and K. Kadowaki, Continuous  $30\ \mu\text{W}$  terahertz source by a high- $T_c$  superconductor mesa structure, *Appl. Phys. Lett.* **103**, 182601 (2013).
- [31] I. Kawayama, C. Zhang, H. B. Wang, and M. Tonouchi, Study on terahertz emission and optical/terahertz pulse responses with superconductors, *Supercond. Sci. Technol.* **26**, 093002 (2013).
- [32] T. M. Benseman, A. E. Koshelev, W.-K. Kwok, U. Welp, K. Kadowaki, J. R. Cooper, and G. Balakrishnan, The ac Josephson relation and inhomogeneous temperature distributions in large  $\text{Bi}_2\text{Sr}_2\text{CaCu}_2\text{O}_{8+\delta}$  mesas for THz emission, *Supercond. Sci. Technol.* **26**, 085016 (2013).
- [33] T. M. Benseman, K. Gray, A. Koshelev, W.-K. Kwok, U. Welp, H. Minami, K. Kadowaki, and T. Yamamoto, Powerful terahertz emission from  $\text{Bi}_2\text{Sr}_2\text{CaCu}_2\text{O}_{8+\delta}$  mesa arrays, *Appl. Phys. Lett.* **103**, 022602 (2013).
- [34] T. M. Benseman, A. E. Koshelev, W.-K. Kwok, U. Welp, V. K. Vlasko-Vlasov, K. Kadowaki, H. Minami, and C. Watanabe, Direct imaging of hot spots in  $\text{Bi}_2\text{Sr}_2\text{CaCu}_2\text{O}_{8+\delta}$  mesa terahertz sources, *J. Appl. Phys.* **113**, 133902 (2013).
- [35] B. Gross, J. Yuan, D. Y. An, M. Y. Li, N. V. Kinev, X. J. Zhou, M. Ji, Y. Huang, T. Hatano, R. G. Mints, V. P. Koshelets, P. H. Wu, H. B. Wang, D. Koelle, and R. Kleiner, Modeling the linewidth dependence of coherent terahertz emission from intrinsic Josephson junction stacks in the hot-spot regime, *Phys. Rev. B* **88**, 014524 (2013).
- [36] D. Y. An *et al.*, Terahertz emission and detection both based on high- $T_c$  superconductors: Towards an integrated receiver, *Appl. Phys. Lett.* **102**, 092601 (2013).
- [37] F. Turkoglu, L. Ozyuzer, H. Koseoglu, Y. Demirhan, S. Preu, S. Malzer, Y. Simsek, H. B. Wang, and P. Müller, Emission of the THz waves from large area mesas of superconducting  $\text{Bi}_2\text{Sr}_2\text{CaCu}_2\text{O}_{8+\delta}$  by the injection of spin polarized current, *Physica (Amsterdam)* **491C**, 7 (2013).
- [38] K. Kadowaki, M. Tsujimoto, K. Delfanzari, T. Kitamura, M. Sawamura, H. Asai, T. Yamamoto, K. Ishida, C. Watanabe, and S. Sekimoto, Quantum terahertz electronics

- (QTE) using coherent radiation from high temperature superconducting  $\text{Bi}_2\text{Sr}_2\text{CaCu}_2\text{O}_{8+\delta}$  intrinsic Josephson junctions, *Physica (Amsterdam)* **491C**, 2 (2013).
- [39] H. Minami, C. Watanabe, K. Sato, S. Sekimoto, T. Yamamoto, T. Kashiwagi, R. A. Klemm, and K. Kadowaki, Local SiC photoluminescence evidence of hot spot formation and sub-THz coherent emission from a rectangular  $\text{Bi}_2\text{Sr}_2\text{CaCu}_2\text{O}_{8+\delta}$  mesa, *Phys. Rev. B* **89**, 054503 (2014).
- [40] T. Kashiwagi, K. Nakade, B. Markovi, Y. Saiwai, H. Minami, T. Kitamura, C. Watanabe, K. Ishida, S. Sekimoto, K. Asanuma, T. Yasui, Y. Shibano, M. Tsujimoto, T. Yamamoto, J. Mirkovi, and K. Kadowaki, Reflection type of terahertz imaging system using a high- $T_c$  superconducting oscillator, *Appl. Phys. Lett.* **104**, 022601 (2014).
- [41] T. Kashiwagi, K. Nakade, Y. Saiwai, H. Minami, T. Kitamura, C. Watanabe, K. Ishida, S. Sekimoto, K. Asanuma, T. Yasui, Y. Shibano, M. Tsujimoto, T. Yamamoto, B. Markovi, J. Mirkovi, R. A. Klemm, and K. Kadowaki, Computed tomography image using sub-terahertz waves generated from a high- $T_c$  superconducting intrinsic Josephson junction oscillator, *Appl. Phys. Lett.* **104**, 082603 (2014).
- [42] A. Grib and P. Seidel, The influence of external separate heating on the synchronization of Josephson junctions, *Phys. Status Solidi B* **251**, 1040 (2014).
- [43] M. Ji, J. Yuan, B. Gross, F. Rudau, D. Y. An, M. Y. Li, X. J. Zhou, Y. Huang, H. C. Sun, Q. Zhu, J. Li, N. Kinev, T. Hatano, V. P. Koshelets, D. Koelle, R. Kleiner, W. W. Xu, B. B. Jin, H. B. Wang, and P. H. Wu,  $\text{Bi}_2\text{Sr}_2\text{CaCu}_2\text{O}_8$  intrinsic Josephson junction stacks with improved cooling: Coherent emission above 1 THz, *Appl. Phys. Lett.* **105**, 122602 (2014).
- [44] M. Tsujimoto, H. Kambara, Y. Maeda, Y. Yoshioka, Y. Nakagawa, and I. Kakeya, Dynamic Control of Temperature Distributions in Stacks of Intrinsic Josephson Junctions in  $\text{Bi}_2\text{Sr}_2\text{CaCu}_2\text{O}_{8+\delta}$  for Intense Terahertz Radiation, *Phys. Rev. Applied* **2**, 044016 (2014).
- [45] T. Kitamura, T. Kashiwagi, T. Yamamoto, M. Tsujimoto, C. Watanabe, K. Ishida, S. Sekimoto, K. Asanuma, T. Yasui, K. Nakade, Y. Shibano, Y. Saiwai, H. Minami, R. A. Klemm, and K. Kadowaki, Broadly tunable, high-power terahertz radiation up to 73 K from a stand-alone  $\text{Bi}_2\text{Sr}_2\text{CaCu}_2\text{O}_{8+\delta}$  mesa, *Appl. Phys. Lett.* **105**, 202603 (2014).
- [46] S. S. Andrews and S. G. Boxer, A liquid nitrogen immersion cryostat for optical measurements, *Rev. Sci. Instrum.* **71**, 3567 (2000).
- [47] H. J. M. ter Brake and G. F. M. Wiegerinck, Low-power cryocooler survey, *Cryogenics* **42**, 705 (2002).
- [48] O. Mitrofanov, T. Tan, P. R. Mark, B. Bowden, and J. A. Harrington, Waveguide mode imaging and dispersion analysis with terahertz near-field microscopy, *Appl. Phys. Lett.* **94**, 171104 (2009).
- [49] O. Mitrofanov, R. James, F. A. Fernández, T. K. Mavrogordatos, and J. A. Harrington, Reducing transmission losses in hollow THz waveguides, *IEEE Trans. THz Sci. Technol.* **1**, 124 (2011).
- [50] H. Eisele, M. Naftaly, and J. R. Fletcher, A simple interferometer for the characterization of sources at terahertz frequencies, *Meas. Sci. Technol.* **18**, 2623 (2007).
- [51] T. Watanabe, T. Fujii, and A. Matsuda, Anisotropic Resistivities of Precisely Oxygen Controlled Single-Crystal  $\text{Bi}_2\text{Sr}_2\text{CaCu}_2\text{O}_{8+\delta}$ : Systematic Study on “Spin Gap” Effect, *Phys. Rev. Lett.* **79**, 2113 (1997).